Applied Mathematics Letters 127 (2022) 107848

Contents lists available at ScienceDirect

Applied Mathematics Letters

www.elsevier.com/locate/aml

An energy stable finite difference method for anisotropic surface diffusion on closed curves

Ming-Chih Lai [a], Sangbeom Park [b,1], Yunchang Seol [b,*]

[a] *Department of Applied Mathematics, National Yang Ming Chiao Tung University, 1001 Ta Hsueh Road, Hsinchu 30010, Taiwan*
[b] *Department of Mathematics, Kyungpook National University, Daegu 41566, Republic of Korea*

ARTICLE INFO

Article history:
Received 8 October 2021
Received in revised form 7 December 2021
Accepted 7 December 2021
Available online 14 December 2021

Keywords:
Anisotropic surface diffusion
Finite difference method
Energy stable scheme

ABSTRACT

In this paper, we develop an energy stable finite difference method for the problem of curve motion under anisotropic surface diffusion. The motion of curve by anisotropic surface diffusion is governed by the fourth-order (highly nonlinear) geometric evolution equation. As in Li and Bao (2021), we first split the fourth-order evolution equation into two second-order equations, where the position vector of curve and the weighted curvature are treated as unknowns. Instead of using the arclength parameter, we introduce a Lagrangian coordinate parameter such that a closed curve can be parametrized over a fixed interval so that the equations can be represented using the new parameter. We then propose a linearly semi-implicit finite difference method to discretize these two equations, and prove that the scheme satisfies discrete energy dissipation so it is energy stable under suitable condition on the anisotropic surface energy. To show the applicability of our present method, we perform several numerical tests on various initial curves and different anisotropic energies. The numerical results show that our scheme is indeed energy dissipative and conserves even the total area well.

1. Introduction

In this paper, we introduce an energy stable finite difference method for motion of closed curves by *anisotropic* surface diffusion. Diffusion process on surface or interface is an important and ubiquitous phenomenon involved with the motion of atoms and molecules over solid surface [1, Ch. 13]. This problem is an important transport mechanism and arises in various applications of surface phase formation, solid-state physics, materials science, and computational geometry [2–5]. For example, a growing crystalline film is an important ingredient for several applications on a nanoscale, and the equilibrium shape of crystals is a classic problem in materials science.

* Corresponding author.
E-mail addresses: mclai@math.nctu.edu.tw (M.-C. Lai), piaoxf76@hanmail.net (S. Park), ycseol@knu.ac.kr (Y. Seol).
[1] Earlier known as Xiangfan Piao.

https://doi.org/10.1016/j.aml.2021.107848
0893-9659/

Based on Nernst–Einstein relation, Mullins in [6] firstly proposed a mathematical formulation for isotropic surface diffusion to study the evolution of grain boundaries, where a thermal groove can be developed progressively due to the diffusion of atoms along the interface. In other words, the evolution of phase interfaces is controlled by mass diffusion within the interfacial surface. Later in [2], it was extended to anisotropic surface diffusion in the context of rational thermodynamics. In addition to thermal grooving, other applications include intergranular voids in microelectric device [7], epitaxial growth [8], and deformation of images [4] (see also references cited therein). Theoretical studies on this problem can be found in [9] and numerical studies in [7,10–13]. In the language of differential geometry, for an evolving closed curve in $\mathbb{R}^2$, motion by *isotropic* surface diffusion as a special case is governed by the fourth-order geometric evolution law

$$\mathbf{X}_t = \kappa_{ss}\mathbf{n}, \tag{1}$$

meaning that a curve moves in normal direction by the surface Laplacian of curvature, refer to the next section for detailed notations.

Since anisotropic process is more common in reality, anisotropic surface diffusion as an extension of the isotropic case has been further studied recently. It was found that the anisotropic diffusion occurs conventionally by different atomic structures on surface and step structure of surface [1]. To model this, a weighted curvature μ replacing κ in Eq. (1) is introduced [14], see Eq. (3). Such model is extensively employed to investigate thin film evolution in solid-state dewetting problems [15]. Some numerical studies with several anisotropic surface energies are presented in [11,13,14].

In solving the isotropic surface diffusion (1), a novel idea is introduced in [10], wherein four unknowns such as scalar curvature, curvature vector, scalar normal velocity, and vector normal velocity are used to develop an energy stable scheme. Later in [12], still preserving the energy stability, this method is tailored by separating Eq. (1) into two equations such as

$$\mathbf{n}\cdot\mathbf{X}_t = \kappa_{ss} \quad \text{and} \quad \kappa\mathbf{n} = -\mathbf{X}_{ss}, \tag{2}$$

where the position vector $\mathbf{X}$ and the curvature κ are defined as two unknowns. We note that the second equation is a well-known identity in differential geometry, namely, the surface Laplacian of position vector is the minus of (mean) curvature normal vector. A similar approach is adopted to anisotropic case in parametric finite element framework in [14].

To solve surface diffusion problems, since the evolution law (1) is written in the context of differential geometry, most of the numerical methods listed above satisfying energy stability are naturally based on surface finite element approach in Lagrangian description. As to grid-based Eulerian methods, one can refer to [16] for level-set approach which requires small time step to enforce the energy stability, and [17] for phase-field approach devised by using invariant energy quadratization method under isotropic surface energy. In this paper, motivated by the energy-stable parametric finite element method proposed by Li and Bao in [14], we propose a finite difference method for (weakly) anisotropic surface diffusion which not only satisfies the property of unconditional energy stability, but also generates a linear system as simple as possible with unknowns in Lagrangian coordinates.

2. Mathematical model

We consider a sufficiently smooth closed curve $\Gamma(t)$ immersed in two dimensional plane. This curve is represented by $\Gamma(t) = \{\mathbf{X}(s,t) = (X(s,t), Y(s,t))\}$, where t is the time and s is the arclength parameterization. As studied in [14], the governing equation for the motion of Γ under anisotropic surface diffusion is given by

$$\mathbf{X}_t = \mu_{ss}\mathbf{n}, \quad \text{and} \quad \mu = (\gamma(\theta) + \gamma''(\theta))\kappa, \tag{3}$$

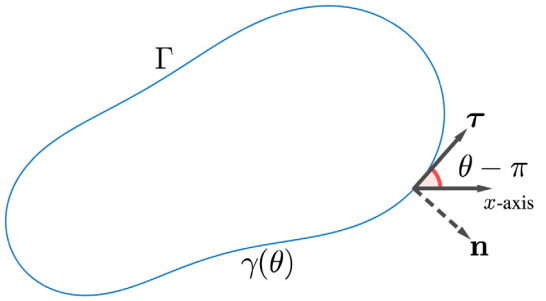

Fig. 1. The problem setup of anisotropic surface diffusion on the curve Γ, where γ is the surface energy, $\boldsymbol{\tau}$ is the tangent vector, and $\mathbf{n}$ is the outward normal vector. The increasing arclength direction is along the counterclockwise direction.

where γ is the dimensionless positive surface energy, κ is the curvature, and $\mathbf{n}$ is the outward unit normal vector. The subscripts of a function denotes its respective partial derivatives. We also denote the unit tangent vector by $\boldsymbol{\tau} = \mathbf{X}_s = (X_s, Y_s)$, and the tangent angle between $\boldsymbol{\tau}$ and the negative horizontal axis by θ. More specifically, the angle is defined by $\tan(\theta - \pi) = \frac{Y_s}{X_s}$, where π is subtracted for comparison purpose with the notations used in [14], see the illustration in Fig. 1. We conventionally use the increasing arclength direction as the counterclockwise direction. Also, by introducing the clockwise rotation of a vector by $\pi/2$, we denote the perpendicular vector of a vector $\mathbf{u} = (u, v)$ by $\mathbf{u}^\perp = (v, -u)$. In such way, the perpendicular vector of unit tangent vector $\mathbf{X}_s$ on the curve is exactly equal to unit outward normal vector $\mathbf{n}$ as $\mathbf{X}_s^\perp = \mathbf{n}$. Notice that, when $\gamma = 1$, Eq. (3) reduces to the isotropic case (1).

Recalling that $\kappa = \theta_s$, $\boldsymbol{\tau}_s = \mathbf{X}_{ss} = -\kappa\mathbf{n}$, and $\mathbf{n}_s = \kappa\boldsymbol{\tau}$ on a plane curve, we have

$$\mu\mathbf{n} = -\left(\gamma(\theta)\mathbf{X}_s - \gamma'(\theta)\mathbf{X}_s^\perp\right)_s.$$

The above equality is derived in [14] where the increasing directions of arclength and angle are opposite from ours.

Using the above equality, the fourth-order geometric evolution equation (3) can be recast by two coupled second-order equations similar to Eq. (2) as

$$\mathbf{n} \cdot \mathbf{X}_t = \mu_{ss}, \tag{4}$$

$$\mu\mathbf{n} = -\left(\gamma(\theta)\mathbf{X}_s - \gamma'(\theta)\mathbf{X}_s^\perp\right)_s. \tag{5}$$

In this paper, we will use the above formulation instead of Eq. (3) as in [12,14] for finite element approach.

Before to proceed, we introduce Lagrangian parameter α such that a closed curve $\Gamma(t) = \{\mathbf{X}(\alpha, t) = (X(\alpha, t), Y(\alpha, t))\}$ can be parametrized over a fixed interval $[0, 2\pi]$ rather than the changing arclength parameter. However, the both parameters can be linked by the arclength element $\mathrm{d}s = |\mathbf{X}_\alpha|\mathrm{d}\alpha = \sqrt{X_\alpha^2 + Y_\alpha^2}\,\mathrm{d}\alpha$, and the derivative $\mathbf{X}_s = \mathbf{X}_\alpha/|\mathbf{X}_\alpha|$. The dynamics of anisotropic surface diffusion has two inherent properties; namely, the total area conservation and energy dissipation. The first property can be easily derived by applying integration by parts over a closed curve Γ as

$$\frac{\mathrm{d}A}{\mathrm{d}t} = \int_\Gamma \mathbf{X}_t \cdot \mathbf{n}\,\mathrm{d}s = \int_\Gamma \mu_{ss}\,\mathrm{d}s = 0.$$

For the total surface energy $E(t) = \int_\Gamma \gamma(\theta)\,\mathrm{d}s$, its rate of change can be obtained as [14]

$$\frac{\mathrm{d}E}{\mathrm{d}t} = -\int_\Gamma \mu_s^2\,\mathrm{d}s \le 0.$$

This shows that the energy E always dissipates in continuous sense. In next section, motivated from this property, we present an energy stable finite difference method that preserves the energy dissipation in discrete sense.

3. An energy stable scheme for anisotropic surface diffusion

As mentioned earlier, we introduce a Lagrangian coordinate $\alpha \in [0, 2\pi]$ along the closed curve $\Gamma(t) = \{\mathbf{X}(\alpha, t) = (X(\alpha, t), Y(\alpha, t))\}$ so that all geometrical quantities and solution variables can be defined on this coordinate. Now the unit tangent can be rewritten as $\boldsymbol{\tau} = \mathbf{X}_\alpha/|\mathbf{X}_\alpha| = (X_\alpha, Y_\alpha)/|\mathbf{X}_\alpha|$ and the outward normal vector $\mathbf{n} = \mathbf{X}_\alpha^\perp/|\mathbf{X}_\alpha| = (Y_\alpha, -X_\alpha)/|\mathbf{X}_\alpha|$. The partial derivative with respect to s is $\frac{\partial}{\partial s} = \frac{1}{|\mathbf{X}_\alpha|}\frac{\partial}{\partial \alpha}$. Based on these notations, one can rewrite Eqs. (4)–(5) as the following

$$\frac{\mathbf{X}_\alpha^\perp}{|\mathbf{X}_\alpha|} \cdot \mathbf{X}_t = \frac{1}{|\mathbf{X}_\alpha|}\frac{\partial}{\partial \alpha}\left(\frac{1}{|\mathbf{X}_\alpha|}\frac{\partial \mu}{\partial \alpha}\right),$$
$$\mu \frac{\mathbf{X}_\alpha^\perp}{|\mathbf{X}_\alpha|} = -\frac{1}{|\mathbf{X}_\alpha|}\frac{\partial}{\partial \alpha}\left(\gamma(\theta)\frac{\mathbf{X}_\alpha}{|\mathbf{X}_\alpha|} - \gamma'(\theta)\frac{\mathbf{X}_\alpha^\perp}{|\mathbf{X}_\alpha|}\right).$$

The above equations can be simplified further as

$$\mathbf{X}_\alpha^\perp \cdot \mathbf{X}_t = \frac{\partial}{\partial \alpha}\left(\frac{1}{|\mathbf{X}_\alpha|}\frac{\partial \mu}{\partial \alpha}\right), \tag{6}$$
$$\mu \mathbf{X}_\alpha^\perp = -\frac{\partial}{\partial \alpha}\left(\gamma(\theta)\frac{\mathbf{X}_\alpha}{|\mathbf{X}_\alpha|} - \gamma'(\theta)\frac{\mathbf{X}_\alpha^\perp}{|\mathbf{X}_\alpha|}\right). \tag{7}$$

Next, we aim to discretize Eqs. (6)–(7). We first layout a uniform mesh grid points $\alpha_i = i\Delta\alpha, i = 0, 1, 2 \ldots N$ with mesh with $\Delta\alpha = 2\pi/N$ in α coordinate along the initial closed curve $\Gamma(0)$. Note that, due to periodicity, we have $\alpha_0 = \alpha_N$. Since the centered difference is used, we also define the "half-integer" points at $\alpha_{i+1/2} = (i + 1/2)\Delta\alpha$. It is very interesting and novel to see that in above α coordinate formulation in Eqs. (6)–(7), the term $\Delta\alpha$ used in finite difference approximations for the derivatives of α can be completely dropped out without changing the approximations. This is another advantage of using α coordinate formulation for the sake of notational simplicity. With that in mind, for a discrete function f, we define the difference operators by

$$\Delta f_{i+1/2} = f_{i+1} - f_i \quad \text{and} \quad \Delta f_i = (f_{i+1} - f_{i-1})/2, \tag{8}$$

where the subscript index i is represented that the function is defined at α_i. For instance, the perpendicular vectors are discretized as

$$(\Delta \mathbf{X}_i)^\perp = (\Delta Y_i, -\Delta X_i) = \left(\frac{Y_{i+1} - Y_{i-1}}{2}, -\frac{X_{i+1} - X_{i-1}}{2}\right)$$

and

$$\left(\Delta \mathbf{X}_{i+1/2}\right)^\perp = \left(\Delta Y_{i+1/2}, -\Delta X_{i+1/2}\right) = \left(Y_{i+1} - Y_i, -\left(X_{i+1} - X_i\right)\right).$$

Other variables are defined in a similar manner. We also define the discrete surface energy by $\gamma_{i+1/2} \coloneqq \gamma\left(\theta_{i+1/2}\right)$, where the angle is obtained from $\tan\left(\theta_{i+1/2} - \pi\right) = \frac{\Delta Y_{i+1/2}}{\Delta X_{i+1/2}}$. Here the subtraction by π is simply for the identical notation of the angle θ used in [14].

Based on above notations, we now propose a semi-implicit finite difference discretization for Eqs. (6)–(7). Let Δt be the time step size and n be the superscript time step index. The time-marching of the scheme from $(\mathbf{X}^n, \mu^n)$ to $(\mathbf{X}^{n+1}, \mu^{n+1})$ is advanced by

$$(\Delta \mathbf{X}_i^n)^\perp \cdot \frac{\mathbf{X}_i^{n+1} - \mathbf{X}_i^n}{\Delta t} = \frac{\Delta \mu_{i+1/2}^{n+1}}{\left|\Delta \mathbf{X}_{i+1/2}^n\right|} - \frac{\Delta \mu_{i-1/2}^{n+1}}{\left|\Delta \mathbf{X}_{i-1/2}^n\right|}, \tag{9}$$

$$\mu_i^{n+1}(\Delta \mathbf{X}_i^n)^\perp = -\frac{\gamma_{i+1/2}^n \Delta \mathbf{X}_{i+1/2}^{n+1} - \gamma'^n_{i+1/2}\left(\Delta \mathbf{X}_{i+1/2}^{n+1}\right)^\perp}{\left|\Delta \mathbf{X}_{i+1/2}^n\right|} + \frac{\gamma_{i-1/2}^n \Delta \mathbf{X}_{i-1/2}^{n+1} - \gamma'^n_{i-1/2}\left(\Delta \mathbf{X}_{i-1/2}^{n+1}\right)^\perp}{\left|\Delta \mathbf{X}_{i-1/2}^n\right|}. \tag{10}$$

One can immediately see that the space (α coordinate) discretization is centered difference while the time discretization is simply Euler method. Meanwhile, the scheme is completely linear despite the original Eqs. (6)–(7) are non-linear. This results a linear system $A\mathbf{x} = \mathbf{b}$ with unknowns $\mathbf{x} = (X^{n+1}, Y^{n+1}, \mu^{n+1})$ which can be solved quite easily.

3.1. Well-posedness and discrete energy dissipation

Here we shall prove the present scheme Eqs. (9)–(10) is well-posed and unconditionally energy stable under some suitable condition on the surface energy γ. The discrete energy at nth time step E^n is defined by

$$E^n = \sum_{i=1}^{N} \gamma^n_{i+1/2} \left| \Delta \mathbf{X}^n_{i+1/2} \right|, \tag{11}$$

which is an integral approximation of the continuous energy $E(t) = \int_\Gamma \gamma(\theta)\, \mathrm{d}s = \int_0^{2\pi} \gamma(\theta) |\mathbf{X}_\alpha|\, \mathrm{d}\alpha$. Our goal is to prove the energy is dissipative; that is, $E^{n+1} \le E^n$ for each time step n. Before to proceed, we introduce the discrete version of integration by parts whose proof is straightforward.

Lemma 1 (*Summation by Parts*). *The following relation holds under the periodicity of index i.*

$$\sum_{i=1}^{N} a_{i+1/2}(f_{i+1} - f_i)(g_{i+1} - g_i) = -\sum_{i=1}^{N} \left[a_{i+1/2}(f_{i+1} - f_i) - a_{i-1/2}(f_i - f_{i-1}) \right] g_i$$

or by using the difference operator (8),

$$\sum_{i=1}^{N} a_{i+1/2} \Delta f_{i+1/2} \Delta g_{i+1/2} = -\sum_{i=1}^{N} \left(a_{i+1/2} \Delta f_{i+1/2} - a_{i-1/2} \Delta f_{i-1/2} \right) g_i.$$

To show the well-posedness of our method, let us define the Sobolev spaces under the periodic boundary condition on a curve Γ as

$$\mathbb{X} := H^1([0, 2\pi]) \times H^1([0, 2\pi]) \quad \text{and} \quad \mathbb{K} := H^1([0, 2\pi]),$$

where $H^1([0, 2\pi]) = \{u : [0, 2\pi] \to \mathbb{R} \,|\, u \in L^2([0, 2\pi]), u_\alpha \in L^2([0, 2\pi])\}$ and

$$L^2([0, 2\pi]) = \left\{ u : [0, 2\pi] \to \mathbb{R} \,\middle|\, \int_0^{2\pi} |u(\alpha, t)|^2 |\mathbf{X}_\alpha| \mathrm{d}\alpha < \infty \right\}.$$

On the discrete curve Γ_h, define the necessary finite spaces; $\mathbb{X}^h := \mathbb{K}^h \times \mathbb{K}^h \subset \mathbb{X}$, and $\mathbb{K}^h \subset \mathbb{K}$ is the space of scalar continuous piecewise linear functions which are connected by the values of f_i, $i = 0, 1, 2 \ldots N$. (Note that, the function f can be X, Y, μ defined previously.)

Followed the similar approach ES-PFEM in [14], we now show that our finite difference method proposed in Eqs. (9)–(10) has a unique weak solution in this space.

Theorem 1 (*Well-posedness*). *For each time step n, assume that the following two conditions are satisfied*

(i) at least two vectors of $\left\{ \Delta \mathbf{X}_{i+1/2} \right\}_{i=1}^N$ are not parallel,
(ii) $\min_{i=1,\ldots,N} \left| \Delta \mathbf{X}_{i+1/2} \right| > 0$.

Then the discretizations (9)–(10) are well-posed in a weak sense, i.e., there exists a unique solution $(\mathbf{X}^{n+1}, \mu^{n+1}) \in \mathbb{X}^h \times \mathbb{K}^h$ of the problem defined by

$$\sum_{i=1}^{N} \mathbf{n}^n_i \cdot \frac{\mathbf{X}^{n+1}_i - \mathbf{X}^n_i}{\Delta t} \phi_i |\Delta \mathbf{X}^n_i| = -\sum_{i=1}^{N} \frac{\Delta \mu^{n+1}_{i+1/2}}{\left| \Delta \mathbf{X}^n_{i+1/2} \right|} \frac{\Delta \phi_{i+1/2}}{\left| \Delta \mathbf{X}^n_{i+1/2} \right|} \left| \Delta \mathbf{X}^n_{i+1/2} \right|, \tag{12}$$

$$\sum_{i=1}^{N} \mu_i^{n+1} \mathbf{n}_i^n \cdot \boldsymbol{\omega}_i |\Delta \mathbf{X}_i^n| = \sum_{i=1}^{N} \frac{\gamma_{i+1/2}^n \Delta \mathbf{X}_{i+1/2}^{n+1} - \gamma'^n_{i+1/2} \left(\Delta \mathbf{X}_{i+1/2}^{n+1}\right)^\perp}{\left|\Delta \mathbf{X}_{i+1/2}^n\right|} \cdot \frac{\Delta \boldsymbol{\omega}_{i+1/2}}{\left|\Delta \mathbf{X}_{i+1/2}^n\right|} \left|\Delta \mathbf{X}_{i+1/2}^n\right|, \tag{13}$$

where $\boldsymbol{\omega} \in \mathbb{X}^h$ *and* $\phi \in \mathbb{K}^h$ *are test functions.*

Proof. First, we show that the discrete weak formulation of Eqs. (9)–(10) is given by Eqs. (12)–(13) written above. To do so, we first multiply Eqs. (9) and (10) by ϕ_i and $\boldsymbol{\omega}_i$, respectively. Then by taking summation by parts (Lemma 1) with respect to the periodic index i in a component-wise manner, one can easily obtain Eqs. (12)–(13).

Since the system of equations (12)–(13) is linear, the uniqueness of solution implies the invertibility of system [18, Thm. 3.5.1]. Thus, existence follows from uniqueness. In the viewpoint of linear transformation, the existence of only trivial solution of the homogeneous system is equivalent to one-to-one correspondence. Consequently, to prove the well-posedness of linear system, it is sufficient to show that its homogeneous problem has only zero solution as in [14].

By using $\mathbf{n}_i^n = (\Delta \mathbf{X}_i^n)^\perp / |\Delta \mathbf{X}_i^n|$ and taking $\phi_i = \mu_i^{n+1}$ and $\boldsymbol{\omega}_i = \mathbf{X}_i^{n+1}$, in Eq. (12) we can obtain

$$\sum_{i=1}^{N} (\Delta \mathbf{X}_i^n)^\perp \cdot \mathbf{X}_i^{n+1} \mu_i^{n+1} = -\Delta t \sum_{i=1}^{N} \frac{\left(\Delta \mu_{i+1/2}^{n+1}\right)^2}{\left|\Delta \mathbf{X}_{i+1/2}^n\right|},$$

and in Eq. (13),

$$\begin{aligned}
&\sum_{i=1}^{N} \mu_i^{n+1} (\Delta \mathbf{X}_i^n)^\perp \cdot \mathbf{X}_i^{n+1} \\
&= \sum_{i=1}^{N} \frac{\gamma_{i+1/2}^n \Delta \mathbf{X}_{i+1/2}^{n+1} - \gamma'^n_{i+1/2} \left(\Delta \mathbf{X}_{i+1/2}^{n+1}\right)^\perp}{\left|\Delta \mathbf{X}_{i+1/2}^n\right|} \cdot \Delta \mathbf{X}_{i+1/2}^{n+1} \\
&= \sum_{i=1}^{N} \frac{\gamma_{i+1/2}^n \Delta \mathbf{X}_{i+1/2}^{n+1}}{\left|\Delta \mathbf{X}_{i+1/2}^n\right|} \cdot \Delta \mathbf{X}_{i+1/2}^{n+1} \quad \left(\text{by } \left(\Delta \mathbf{X}_{i+1/2}^{n+1}\right)^\perp \cdot \Delta \mathbf{X}_{i+1/2}^{n+1} = 0\right) \\
&= \sum_{i=1}^{N} \frac{\gamma_{i+1/2}^n \left(\Delta \mathbf{X}_{i+1/2}^{n+1}\right)^2}{\left|\Delta \mathbf{X}_{i+1/2}^n\right|}.
\end{aligned}$$

Combining these two results for $\gamma \geq 0$, we establish

$$0 \leq \sum_{i=1}^{N} \frac{\gamma_{i+1/2}^n \left(\Delta \mathbf{X}_{i+1/2}^{n+1}\right)^2}{\left|\Delta \mathbf{X}_{i+1/2}^n\right|} = \mu_i^{n+1} \sum_{i=1}^{N} (\Delta \mathbf{X}_i^n)^\perp \cdot \mathbf{X}_i^{n+1} = -\Delta t \sum_{i=1}^{N} \frac{\left(\Delta \mu_{i+1/2}^{n+1}\right)^2}{\left|\Delta \mathbf{X}_{i+1/2}^n\right|} \leq 0.$$

This concludes that for all i, it gives $\Delta \mu_{i+1/2}^{n+1} = 0$ and $\Delta \mathbf{X}_{i+1/2}^{n+1} = 0$, thus both variables are constants such as $\mu_{i+1/2}^{n+1} = \mu^c$ and $\mathbf{X}_{i+1/2}^{n+1} = \mathbf{X}^c$. Replacing by these constants into Eqs. (12) and (13) in the homogeneous case, we obtain

$$\sum_{i=1}^{N} \mathbf{n}_i^n \cdot \frac{\mathbf{X}^c}{\Delta t} \phi_i |\Delta \mathbf{X}_i^n| = 0, \quad \forall \phi \in \mathbb{K}^h$$

and

$$\sum_{i=1}^{N} \mu^c \mathbf{n}_i^n \cdot \boldsymbol{\omega}_i |\Delta \mathbf{X}_i^n| = 0, \quad \forall \boldsymbol{\omega} \in \mathbb{X}^h.$$

Under the two assumptions (i) and (ii) and using the result in [12, Thm. 2.1], we can show that both μ^c and $\mathbf{X}^c$ are in fact zero. This completes the proof of well-posedness of our linear system. □

The following main theorem shows that our method is an energy stable scheme.

Theorem 2 (*Discrete Energy Dissipation*)**.** *Under the periodicity of index i, and a generic energy dissipation condition [14] as*

$$2\gamma(\theta) - \gamma(\theta)\cos(\theta-\phi) - \gamma'(\theta)\sin(\theta-\phi) \geq \gamma(\phi), \qquad \forall \theta, \phi \in [-\pi, \pi], \tag{14}$$

the scheme of (9)–(10) is unconditionally energy stable; that is, the scheme satisfies $E^{n+1} \leq E^n$ for each time step n.

Proof. We first start by

$$\begin{aligned}
&\sum_{i=1}^{N} \frac{\gamma^n_{i+1/2}\Delta\mathbf{X}^{n+1}_{i+1/2} - \gamma'^n_{i+1/2}\left(\Delta\mathbf{X}^{n+1}_{i+1/2}\right)^{\perp}}{\left|\Delta\mathbf{X}^n_{i+1/2}\right|} \cdot \left(\Delta\mathbf{X}^{n+1}_{i+1/2} - \Delta\mathbf{X}^n_{i+1/2}\right) + E^n \\
= &\sum_{i=1}^{N} \frac{\gamma^n_{i+1/2}\Delta\mathbf{X}^{n+1}_{i+1/2} - \gamma'^n_{i+1/2}\left(\Delta\mathbf{X}^{n+1}_{i+1/2}\right)^{\perp}}{\left|\Delta\mathbf{X}^n_{i+1/2}\right|} \cdot \left(\Delta\mathbf{X}^{n+1}_{i+1/2} - \Delta\mathbf{X}^n_{i+1/2}\right) + \sum_{i=1}^{N} \gamma^n_{i+1/2}\left|\Delta\mathbf{X}^n_{i+1/2}\right| \\
= &\sum_{i=1}^{N} \frac{1}{\left|\Delta\mathbf{X}^n_{i+1/2}\right|}\left[\left(\gamma^n_{i+1/2}\Delta\mathbf{X}^{n+1}_{i+1/2} - \gamma'^n_{i+1/2}\left(\Delta\mathbf{X}^{n+1}_{i+1/2}\right)^{\perp}\right)\right. \\
&\left. \cdot \left(\Delta\mathbf{X}^{n+1}_{i+1/2} - \Delta\mathbf{X}^n_{i+1/2}\right) + \gamma^n_{i+1/2}\left|\Delta\mathbf{X}^n_{i+1/2}\right|^2\right] \\
= &\sum_{i=1}^{N} \frac{\gamma^n_{i+1/2}}{\left|\Delta\mathbf{X}^n_{i+1/2}\right|}\left(\left|\Delta\mathbf{X}^{n+1}_{i+1/2}\right|^2 - \Delta\mathbf{X}^{n+1}_{i+1/2}\cdot\Delta\mathbf{X}^n_{i+1/2} + \left|\Delta\mathbf{X}^n_{i+1/2}\right|^2\right) \\
&- \frac{\gamma'^n_{i+1/2}}{\left|\Delta\mathbf{X}^n_{i+1/2}\right|}\left[\left(\Delta\mathbf{X}^{n+1}_{i+1/2}\right)^{\perp}\cdot\Delta\mathbf{X}^{n+1}_{i+1/2} - \left(\Delta\mathbf{X}^{n+1}_{i+1/2}\right)^{\perp}\cdot\Delta\mathbf{X}^n_{i+1/2}\right] \\
\geq &\sum_{i=1}^{N} \frac{\gamma^n_{i+1/2}}{\left|\Delta\mathbf{X}^n_{i+1/2}\right|}\left(2\left|\Delta\mathbf{X}^{n+1}_{i+1/2}\right|\left|\Delta\mathbf{X}^n_{i+1/2}\right| - \Delta\mathbf{X}^{n+1}_{i+1/2}\cdot\Delta\mathbf{X}^n_{i+1/2}\right) \\
&+ \frac{\gamma'^n_{i+1/2}}{\left|\Delta\mathbf{X}^n_{i+1/2}\right|}\left(\Delta\mathbf{X}^{n+1}_{i+1/2}\right)^{\perp}\cdot\Delta\mathbf{X}^n_{i+1/2} \quad (\text{by } a^2+b^2 \geq 2ab \text{ for } a,b\in\mathbb{R}) \\
= &\sum_{i=1}^{N} \frac{\gamma^n_{i+1/2}}{\left|\Delta\mathbf{X}^n_{i+1/2}\right|}\left[2\left|\Delta\mathbf{X}^{n+1}_{i+1/2}\right|\left|\Delta\mathbf{X}^n_{i+1/2}\right| - \left|\Delta\mathbf{X}^{n+1}_{i+1/2}\right|\left|\Delta\mathbf{X}^n_{i+1/2}\right|\cos\left(\theta^{n+1}_{i+1/2} - \theta^n_{i+1/2}\right)\right] \\
&+ \frac{\gamma'^n_{i+1/2}}{\left|\Delta\mathbf{X}^n_{i+1/2}\right|}\left|\Delta\mathbf{X}^{n+1}_{i+1/2}\right|\left|\Delta\mathbf{X}^n_{i+1/2}\right|\cos\left(\theta^{n+1}_{i+1/2} - \tfrac{\pi}{2} - \theta^n_{i+1/2}\right) \\
&\left(\text{where } \theta^{n+1}_{i+1/2} - \theta^n_{i+1/2} \text{ equals to the angle between } \Delta\mathbf{X}^{n+1}_{i+1/2} \text{ and } \Delta\mathbf{X}^n_{i+1/2}\right) \\
= &\sum_{i=1}^{N} \left|\Delta\mathbf{X}^{n+1}_{i+1/2}\right|\left[2\gamma^n_{i+1/2} - \gamma^n_{i+1/2}\cos\left(\theta^{n+1}_{i+1/2} - \theta^n_{i+1/2}\right) + \gamma'^n_{i+1/2}\sin\left(\theta^{n+1}_{i+1/2} - \theta^n_{i+1/2}\right)\right] \\
= &\sum_{i=1}^{N} \left|\Delta\mathbf{X}^{n+1}_{i+1/2}\right|\left[2\gamma^n_{i+1/2} - \gamma^n_{i+1/2}\cos\left(\theta^n_{i+1/2} - \theta^{n+1}_{i+1/2}\right) - \gamma'^n_{i+1/2}\sin\left(\theta^n_{i+1/2} - \theta^{n+1}_{i+1/2}\right)\right] \\
\geq &\sum_{i=1}^{N} \gamma^{n+1}_{i+1/2}\left|\Delta\mathbf{X}^{n+1}_{i+1/2}\right| \quad (\text{by the energy dissipation condition (14)}) \\
= &\ E^{n+1}.
\end{aligned}$$

From this, we can derive further as

$$
\begin{aligned}
& E^{n+1} - E^n \\
\leq\ & \sum_{i=1}^{N} \frac{\gamma_{i+1/2}^n \Delta \mathbf{X}_{i+1/2}^{n+1} - \gamma'^n_{i+1/2} \left(\Delta \mathbf{X}_{i+1/2}^{n+1}\right)^{\perp}}{\left|\Delta \mathbf{X}_{i+1/2}^n\right|} \cdot \left(\Delta \mathbf{X}_{i+1/2}^{n+1} - \Delta \mathbf{X}_{i+1/2}^n\right) \\
=\ & -\sum_{i=1}^{N} \left(\frac{\gamma_{i+1/2}^n \Delta \mathbf{X}_{i+1/2}^{n+1} - \gamma'^n_{i+1/2} \left(\Delta \mathbf{X}_{i+1/2}^{n+1}\right)^{\perp}}{\left|\Delta \mathbf{X}_{i+1/2}^n\right|} - \frac{\gamma_{i-1/2}^n \Delta \mathbf{X}_{i-1/2}^{n+1} - \gamma'^n_{i-1/2} \left(\Delta \mathbf{X}_{i-1/2}^{n+1}\right)^{\perp}}{\left|\Delta \mathbf{X}_{i-1/2}^n\right|} \right) \\
& \cdot \left(\mathbf{X}_i^{n+1} - \mathbf{X}_i^n\right) \quad \text{(by applying Lemma 1 component-wisely)} \\
=\ & \textstyle\sum_{i=1}^{N} \mu_i^{n+1} (\Delta \mathbf{X}_i^n)^{\perp} \cdot \left(\mathbf{X}_i^{n+1} - \mathbf{X}_i^n\right) \quad \text{(by Eq. (10))} \\
=\ & \sum_{i=1}^{N} \mu_i^{n+1} \Delta t \left(\frac{\Delta \mu_{i+1/2}^{n+1}}{\left|\Delta \mathbf{X}_{i+1/2}^n\right|} - \frac{\Delta \mu_{i-1/2}^{n+1}}{\left|\Delta \mathbf{X}_{i-1/2}^n\right|} \right) \quad \text{(by Eq. (9))} \\
=\ & -\Delta t \sum_{i=1}^{N} \Delta \mu_{i+1/2}^{n+1} \frac{\Delta \mu_{i+1/2}^{n+1}}{\left|\Delta \mathbf{X}_{i+1/2}^n\right|} \quad \text{(by Lemma 1)} \\
=\ & -\Delta t \sum_{i=1}^{N} \frac{\left(\Delta \mu_{i+1/2}^{n+1}\right)^2}{\left|\Delta \mathbf{X}_{i+1/2}^n\right|} \leq 0,
\end{aligned}
$$

which completes the proof. □

This theorem ensures that our scheme in Eqs. (6)–(7) is an energy stable finite difference method for the curve motion driven by anisotropic surface diffusion. The governing equation for surface diffusion is expressed by a fourth-order geometric equation, wherein the unknown is the position vector of curve. As in some work in literature, we use a geometric identity as the second equation by taking weighted curvature as an extra unknown so the original fourth-order partial differential equation becomes two second-order equations. We introduce a Lagrangian coordinate parameter such that a closed curve can be parametrized over a fixed interval so the equations can be represented using the new parameter instead of using the changing arclength parameter. Then, we propose a semi-implicit finite difference method for those two equations and prove that the scheme is unconditionally energy stable under a generic energy dissipative condition on the surface energy. More importantly, the present numerical scheme results in a linear system for two unknowns despite the fact that the original partial differential equation is non-linear. As future work, the present finite difference method can be coupled with an equi-arclength mesh control mechanism [19] so the mesh quality can be significantly improved while preserving the original dynamics of surface diffusion. Another promising future work is the development of a structure-preserving finite difference method which simultaneously satisfies area conservation and energy dissipation in discrete sense as in [20]. Meanwhile, it is also possible to extend the study for the evolution of open curves with proper boundary conditions for solid-state dewetting problems as in [11,14,21]. However, careful discretization near the boundary must be taken in order to preserve energy dissipation. In the next section, various numerical experiments are performed to show the applicability of our finite difference method satisfying unconditional energy stability.

4. Numerical results

We perform a series of numerical tests for the motion of curve under anisotropic surface diffusion. We begin by checking the convergence rate of developed scheme (9)–(10) for the curve position vector $\mathbf{X}$ and the weighted curvature (or chemical potential) μ. We then study the evolving dynamics of closed curves under anisotropic surface energy.

Table 1
Convergence analysis for anisotropic surface diffusion with energy $\gamma(\theta) = 1 + 0.1\cos(3\theta)$ at two different times $t = 0.0078$ and 0.0156.

N	$\|\mathbf{X}_N - \mathbf{X}_{2N}\|_2$	Rate	$\|\mu_N - \mu_{2N}\|_2$	Rate
	$(t = 0.0078)$			
64	3.996×10^{-2}	–	1.805×10^{-1}	–
128	2.261×10^{-2}	0.82	7.537×10^{-2}	1.26
256	1.221×10^{-2}	0.88	3.245×10^{-2}	1.21
512	7.467×10^{-3}	0.71	1.970×10^{-2}	0.71
	$(t = 0.0156)$			
64	5.071×10^{-2}	–	1.069×10^{-1}	–
128	2.669×10^{-2}	0.92	5.847×10^{-2}	0.87
256	1.483×10^{-2}	0.84	2.346×10^{-2}	1.31
512	8.485×10^{-3}	0.80	1.073×10^{-2}	1.12

4.1. Convergence test

As the first test, we check the numerical accuracy of our method presented in Section 3. As mentioned before, the curve is discretized by the N-number of points with the Lagrangian mesh width $\Delta\alpha = 2\pi/N$. We define the L_2-norm of the position vector $\mathbf{X}_N$ by $\|\mathbf{X}_N\|_2 := \left(\sum_{i=1}^{N} |\mathbf{X}_{N,i}|^2 \, \Delta s_{N,i}\right)^{1/2}$, where the arclength element is $\Delta s_{N,i} = \left(|\Delta\mathbf{X}_{N,i+1/2}| + |\Delta\mathbf{X}_{N,i-1/2}|\right)/2$. So the error of $\mathbf{X}$ between two resolutions associated with N and $2N$ can be obtained from

$$\|\mathbf{X}_N - \mathbf{X}_{2N}\|_2 = \left(\sum_{i=1}^{N} |\mathbf{X}_{N,i} - \widetilde{\mathbf{X}_{2N,i}}|^2 \, \Delta s_{N,i}\right)^{1/2},$$

where $\widetilde{\mathbf{X}_{2N}}$ is the N-sized data of $\mathbf{X}_{2N}$ projected onto $\mathbf{X}_N$. The convergence rate is then computed by

$$\text{Rate} = \log_2\left(\frac{\|\mathbf{X}_N - \mathbf{X}_{2N}\|_2}{\|\mathbf{X}_{2N} - \mathbf{X}_{4N}\|_2}\right).$$

The error and convergence rate for the weighted curvature μ are computed in a similar manner. Here, the initial curve is chosen as a complex one in [22] with the parametric form $(X, Y) = (\cos\alpha,\ 0.5\sin\alpha + \sin(\cos\alpha) + (0.2 + \sin\alpha\sin^2(3\alpha))\sin\alpha)$ and the time step is chosen as $\Delta t = 1/(32N)$. The anisotropic energy is chosen as $\gamma(\theta) = 1 + 0.1\cos(3\theta)$.

Given an initially complex curve as described above, we increase the number of points N from 64 to 1024 by a factor of two. We compute the L_2 errors of $\mathbf{X}$ and μ at two different times $t = 0.0078$ and 0.0156. As shown in Table 1, we observe that the overall convergence rates for both solution variables $(\mathbf{X}, \mu)$ are roughly close to one. Although the second-order finite difference method is used in space, the overall first-order accuracy can be anticipated since our scheme (9)–(10) uses the first-order backward Euler method in time.

4.2. Effect of anisotropic surface energy

In this subsection, we study the effect of different anisotropic surface energy on motion of curves. We employ two different surface energies as follows.

- $\gamma_1(\theta) = 1 + 0.1\cos(3\theta)$: a 3-fold anisotropic surface energy
- $\gamma_2(\theta) = 1 + 0.05\cos(4\theta)$: a 4-fold anisotropic surface energy

One can refer to [11,14] for more general surface energies. Notice that, the above two energies γ_1 and γ_2 satisfy the generic energy dissipation condition (14) as shown in [14], so the result in Theorem 2

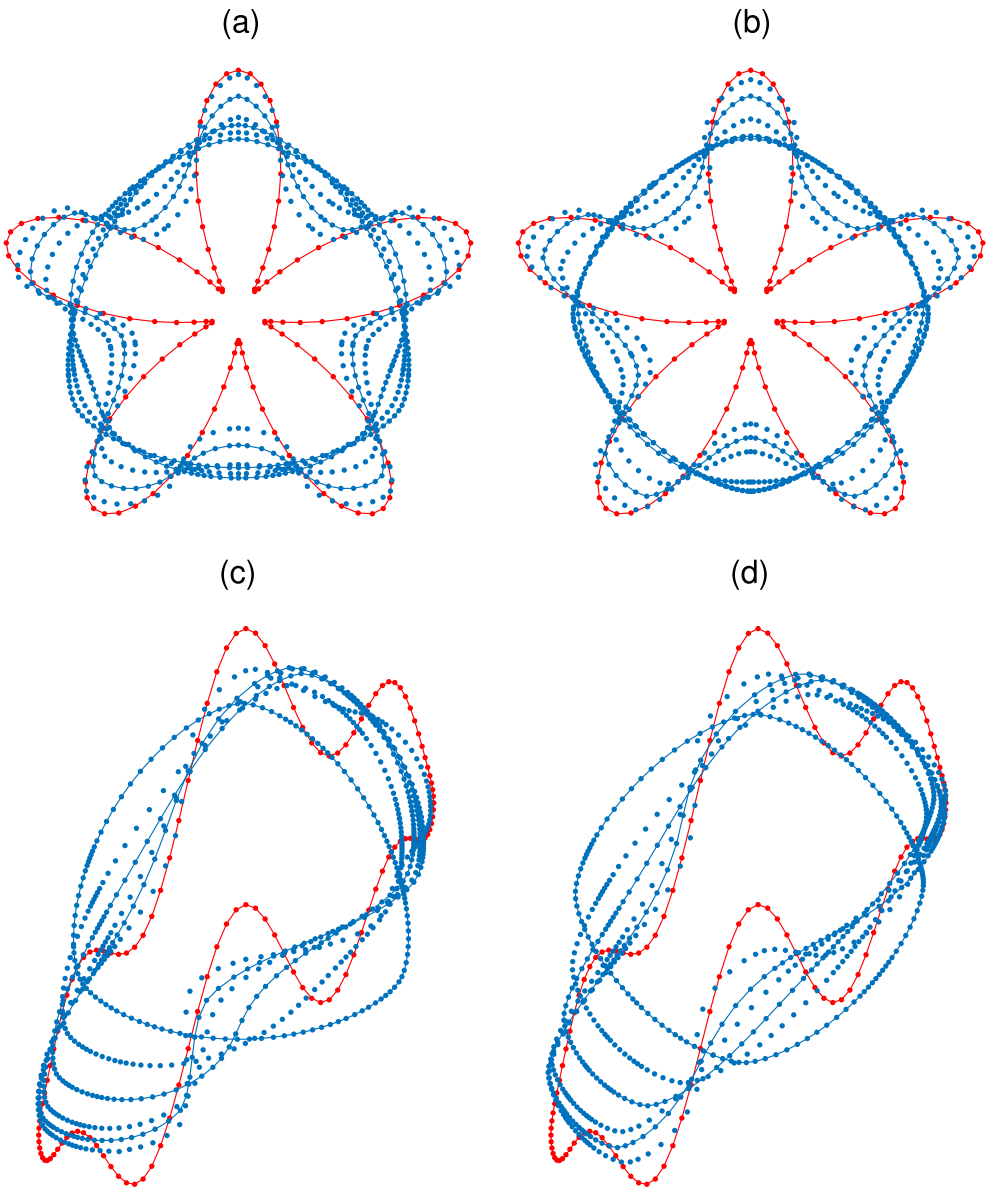

Fig. 2. The motion of curve under anisotropic surface diffusion with 3-fold surface energy $\gamma(\theta) = 1 + 0.1\cos(3\theta)$ in (a,c); and with 4-fold surface energy $\gamma(\theta) = 1 + 0.05\cos(4\theta)$ in (b,d). Two different initial curves are used, namely, (a,b) star-shaped curve; (c,d) complex curve.

can be applied to both cases. To understand their effects more clearly, two different initial curves are chosen; namely, the star-shaped curve $(X, Y) = (1 + 0.8\sin(5\alpha))(\cos\alpha,\ \sin\alpha)$, and the complex curve $(X, Y) = (\cos\alpha,\ 0.5\sin\alpha + \sin(\cos\alpha) + (0.2 + \sin\alpha\sin^2(3\alpha))\sin\alpha)$. We use the grid number $N = 128$ and the time step size is $\Delta t = 1/(32N)$. All simulations are up to time $T = 25/N$ when the equilibrium seems to occur.

In Fig. 2(a,c), the temporal evolution of two curves under the 3-fold anisotropic energy is illustrated. We observe that the high curvature regions are quickly smoothed out in a short time, and then both curves converge to smooth triangles. Once the equilibrium shape is reached, it is unchanged until the final time of simulation. Similar in Fig. 2(b,d), we observe that two curves are again smoothed out quickly, then converge

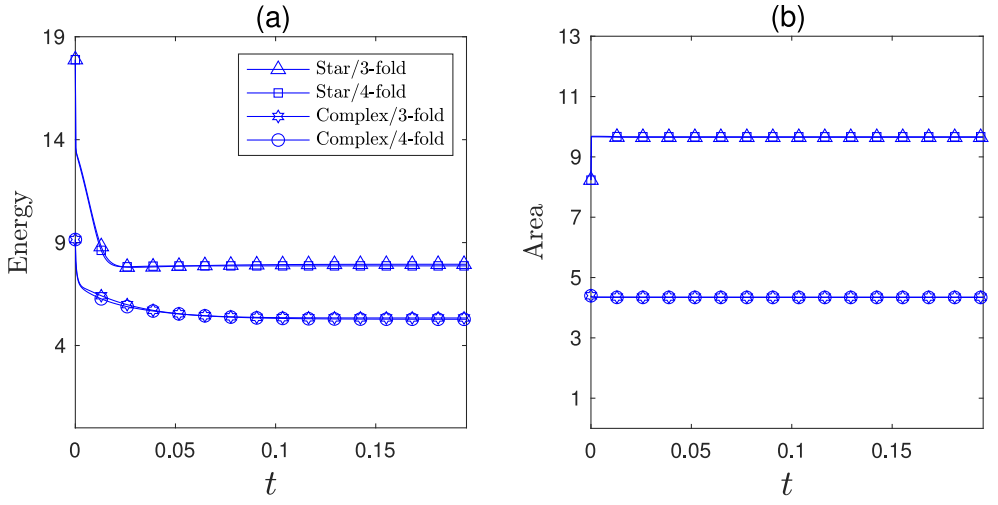

Fig. 3. The temporal evolutions of (a) total energy, and (b) total area, for the curve motion under anisotropic surface diffusion corresponding to Fig. 2.

to smooth diamond shapes and remain unchanged afterwards. In other words, regardless of the initial curve used, the curve motion with a general k-fold anisotropic energy will converge gradually to a smooth k-sided polygon as time goes.

In Fig. 3(a), the temporal evolution of discrete total energy (11) for the four cases corresponding to Fig. 2 is plotted in detail. As expected, the total energy always decreases and remains steady until the final time of simulation which again confirms our theoretical result in Theorem 1. Meanwhile, it is very interesting to see that the energy dissipation for both types of surface energy γ_1 and γ_2 is almost identical for the curves with same initial configuration. In other words, the initial configuration of given curve, rather than the type of energy anisotropy, is more relevant to the energy dissipation property. Fig. 3(b) shows the temporal evolution of total area which shares the same behavior as in Fig. 3(a). In summary, the different k-fold surface anisotropies seem to have negligible effect on the total surface energy and the total area. Besides, the present scheme also conserves the total area quite well.

Acknowledgments

The work of M.-C. Lai was supported in part by Ministry of Science and Technology of Taiwan under research grant MOST-107-2115-M-009-016-MY3 and NCTS, Taiwan. The work of S. Park was supported by the National Research Foundation of Korea (NRF) grand funded by the Korea government (MSIT), South Korea (NRF-2020R1A2C1A01008506). The work of Y. Seol was supported by the basic science research program through the National Research Foundation of Korea (NRF) funded by the Korea government, South Korea (NRF-2020R1A4A1018190).

References

[1] K. Oura, V.G. Lifshits, A.A. Saranin, A.V. Zotov, M. Katayama, Surface Science: An Introduction, Springer-Verlag, Berlin Heidelberg, 2003.
[2] F. Davì, M.E. Gurtin, On the motion of a phase interface by surface diffusion, Z. Angew. Math. Phys. 41 (1990) 782–811.
[3] J.W. Cahn, J.E. Taylor, Surface motion by surface diffusion, Acta Metall. Mater. 42 (1994) 1045–1063.
[4] U. Clarenz, U. Diewald, M. Rumpf, Anisotropic geometric diffusion in surface processing, in: IEEE Proceedings Visualization, 2000, pp. 397-405.
[5] C.V. Thompson, Solid state dewetting of thin films, Annu. Rev. Mater. Res. 42 (2012) 399–434.

[6] W.W. Mullins, Theory of thermal grooving, J. Appl. Phys. 28 (1957) 333–339.
[7] A. Averbuch, M. Israeli, I. Ravve, Electromigration of intergranular voids in metal films for microelectronic interconnects, J. Comput. Phys. 186 (2003) 481–502.
[8] E. Fried, M.E. Gurtin, The role of the configurational force balance in the nonequilibrium epitaxy of films, Mech. Phys. Solids 51 (2003) 487–517.
[9] J. Escher, U.F. Mayer, G. Simonett, The surface diffusion flow for immersed hypersurfaces, SIAM J. Math. Anal 29 (1998) 1419–1433.
[10] E. Bänsch, P. Morin, R.H. Nochetto, A finite element method for surface diffusion: The parametric case, J. Comput. Phys. 203 (2005) 321–343.
[11] W. Bao, W. Jiang, Y. Wang, Q. Zhao, A parametric finite element method for solid-state dewetting problems with anisotropic surface energies, J. Comput. Phys. 330 (2017) 380–400.
[12] J.W. Barrett, H. Garcke, R. Nürnberg, A parametric finite element method for fourth order geometric evolution equations, J. Comput. Phys. 222 (2007) 441–467.
[13] W. Jiang, Q. Zhao, W. Bao, Sharp-interface model for simulating solid-state dewetting in three dimensions, SIAM J. Appl. Math. 80 (4) (2020) 1654–1677.
[14] Y. Li, W. Bao, An energy-stable parametric finite element method for anisotropic surface diffusion, J. Comput. Phys. 446 (2021) 110658.
[15] Y. Wang, W. Jiang, W. Bao, D.J. Srolovitz, Sharp interface model for solid-state dewetting problems with weakly anisotropic surface energies, Phys. Rev. B 91 (2015) 045303.
[16] M. Burger, F. Hauß er, C. Stöcker, A. Voigt, A level set approach to anisotropic flows with curvature regularization, J. Comput. Phys. 225 (2007) 183–205.
[17] Q.-A. Huang, W. Jian, J.Z. Yang, An efficient and unconditionally energy stable scheme for simulating solid-state dewetting of thin films with isotropic surface energy, Commun. Comput. Phys. 26 (2019) 1444–1470.
[18] B.N. Datta, Numerical Methods for Linear Control Systems: Design and Analysis, Academic Press, Cambridge, MA, 2004.
[19] Y. Seol, M.-C. Lai, Spectrally accurate algorithm for points redistribution on closed curves, SIAM J. Sci. Comput. 42 (2020) A3030–A3054.
[20] W. Bao, Q. Zhao, A structure-preserving parametric finite element method for surface diffusion, SIAM J. Numer. Anal. 59 (5) (2021) 2775–2799.
[21] Q. Zhao, W. Jiang, W. Bao, An energy-stable parametric finite element method for simulating solid-state dewetting, IMA J. Numer. Anal. 41 (3) (2021) 2026–2055.
[22] K. Mikula, D. Š.evčovič, Evolution of plane curves driven by a nonlinear function of curvature and anisotropy, SIAM J. Appl. Math 61 (5) (2001) 1473–1501.